Asian Journal of Physical and Chemical Sciences

Volume 10, Issue 4, Page 16-27, 2022; Article no.AJOPACS.94286
ISSN: 2456-7779

Modeling and Validation of Biogas Consumption Prediction in Cook Stove Using a Network Approach

Noufou Bagaya [a*], Issaka Ouédraogo [b], Windé Nongué Daniel Koumbem [a], Younoussa Moussa Baldé [c], Sette Diop [c] and Sié Kam [a]

[a] *Université Joseph KI-ZERBO 03 BP 7021 Ouagadougou 03, Laboratoire d' Energies Thermiques Renouvelables (LETRE), Ouagadougou, Burkina Faso.*

[b] *Institut de Recherche en Sciences Appliquées et Technologies (IRSAT/CNRST) 03 BP 7047 Ouagadougou 03, Département Energie, Ouagadougou, Burkina Faso.*

[c] *Laboratoire des Signaux et systèmes, CNRS- Supélec – Univ. Paris Sud, Plateau de Moulon, 91192 Gif sur Yvette cedex France.*

Authors' contributions

This work was carried out in collaboration among all authors. Author NB wrote the equations and the experimental protocol. IO wrote the first draft of the manuscript. Authors NB and IO implemented the program under Matlab. Authors DWNK and IO managed the analysis of the study and made corrections. Authors YMB and IO managed the bibliographic searches and checked the various calculations. Authors SD and SK checked the modeling and confirmed the discussion. All authors read and approved the final manuscript.

Article Information

DOI: 10.9734/AJOPACS/2022/v10i4187

Open Peer Review History:
This journal follows the Advanced Open Peer Review policy. Identity of the Reviewers, Editor(s) and additional Reviewers, peer review comments, different versions of the manuscript, comments of the editors, etc are available here: https://www.sdiarticle5.com/review-history/94286

Original Research Article

Received: 01/10/2022
Accepted: 03/12/2022
Published: 16/12/2022

Corresponding author: E-mail: nybagaya@gmail.com;

ABSTRACT

This study seeks to propose a new model of hearth for the consumption of biogas produced by a biodigester of 4 m^{-3}. The cylindrical furnace is used to heat an empty pot for 3 hours. To do this, the system is subdivided into two sub-systems, the first is the flame, which heats the bottom of the pot. The latter is the second hottest point. The developed network is composed of 8 isothermal points, interconnected by thermal resistances, each of which represents a particular type of heat transfer mode. The resolution of the system required 8 differential equations. The modeling allowed us to appreciate the temperatures governing the system. The experimental study proves an agreement with the model temperatures. Studies show that the cook stvoe's optimal thickness and height are respectively 18 mm and 09 cm. The heat ide the internal air of the kettle is 220°C and the flame temperature is 900°C. The instantaneous efficiency of the cook stove obtained is 65%. In addition, a validation with literature data to confirm this study with maximmum gap of 5%, therefore its adoption will lead to reducing the consumption of biogas and therefore have a positive impact on the woodcut.

Keywords: Biogas; cook stove; validation; energy performance.

2010 Mathematics Subject Classification: 53C25, 83C05, 57N16.

ABBREVIATIONS

ABBREVIATIONS		
A1...A10	Area surface of the heating	m^2
a,b...j,k	differents points in the stove	$kJ.L^{-1}$
D	biogas flow	$L.s^{-1}$
Cd	coefficent de pertes de charge	Without unit
Cp	Chaleur spefique	W(mK)
h	Heat transfer coefficient	$(W.m^{-2}.K)$
U_{i-j}	Conduction heat transfer	$W.K^{-1}$
m	Mass	kg
PCI	Power Calorific Value	$kJ.L^{-1}$
λ	Thermal conductivity	$(W.m^{-2}.K)$
ρ	Density	kg.m3
Ta...Tk	Température	°C,K
β	coefficient of expansion	$^{\circ}C^{-1}$
Gr	Nombre de grasoft	Without unit
Nu	Number of nussselt	Without unit
F	Form Factor	Sans unite
Ra	Number of Raleigh	Without unit
Pr	Number of Prandtl	Without unit
p	Pression	atm
σ	$5.6.10^{-8}$	$(\mathrm{W.m^2K^4})$
Q,q_{comb}	Quantity of energy	J
η	energy efficiency	%

1 INTRODUCION

Households are the most dominant energy-consuming sector, accounting for around 80% of the country's total energy consumption [1]. According to the population census [2] shows that 76.4% of households in Burkina Faso use firewood and charcoal with a single hearth to cook food. Households using fuels (butane gas and biogas) represent 16.1% in the country. The heavy reliance on the use of single cook stoves which have

a relatively low conversion rate of biomass to energy is one of the factors contributing to the over-consumption of biomass resulting in an increased rate of forest degradation [3]. Butane gas is experiencing disruptions in distribution, which are hampering its adoption by households. Given this situation, researching technologies to improve the conversion of biomass to energy in even a small country can have an overall impact on the economy of available fuel. In this sense, the Burkina Faso government has set up the National Biodigester Program (PNB-BF) to offer an alternative to fuelwood [4]. Thus, optimizing the energy consumption of the household will allow the acceptance of the biodigester technology in a household which can lead to the adoption of biodigesters as the desired goal [5]. This study was motivated by the need to assess stove energy efficiency. The stove prototype is cylindrical in shape with a burner containing a 3.5mm nozzle fed with 60% methane biogas. The study focuses on modeling under **MATLAB** $R2021b$ by the thermal network approach and experimentation. In the end, we will have the optimal dimensions of an energy-efficient cook stove compared to an existing.

2 MATERIALS AND METHODS

2.1 Presentation of the Model

The system is subdivided into two subsystems $\{a, b, c, d, k, h\}$ et $\{d, e, f, g, h\}$ The way it works is that the heat source point exchanges with points (a, b, c, d, h, and k). The greatest exchange is with point (d) which will later become the second hottest point. This last point will exchange vice versa with the points (e, f, g), and the ambient medium (k). Point (d) acts as a bridge between the two subsystems. Conduction was studied between (h) and (a), considering the strong heat coming from the burner at point (a) and the doubled thickness of 14 mm between (a) and (h). The search for the temperature of the internal air of the kettle is the objective of the heating. The physical model and the circuit allowing the discretization of the equations are represented in Fig. 1a and 1b.

2.2 Simplifying Assumptions

Assumptions are adopted to simplify the modeling.

- The airflow is even in the burner
- The heat flux and temperature of each component are uniform at each time step
- The volume of air in the pot is constant
- The temperature of the outdoor air and the fireplace is uniform and the same as that of the floor
- Heat loss around fireplace does not affect room temperature
- No mass transfer is considered
- The derivative is a function of the time in the discretization.

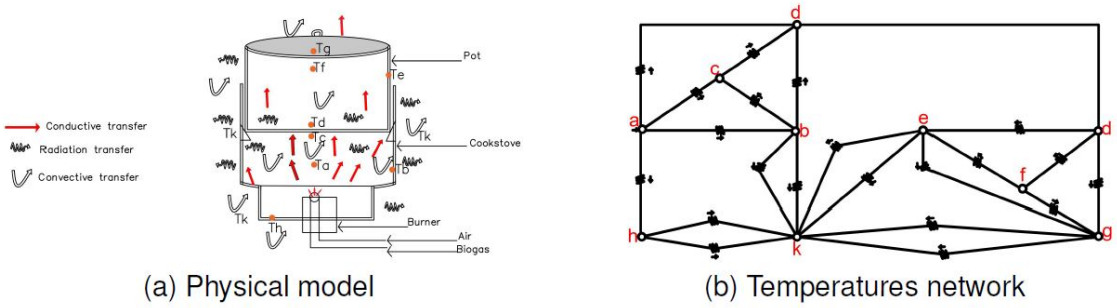

(a) Physical model (b) Temperatures network

Fig. 1. Study model and circuit of thermal network model in the discretization of spots hot

(a) Study cook Stove

(b) Experimentation with the fireplace

Fig. 2. Type of stove and the complete experimentation device

2.3 Stove Presentation

The cook stove is constructed from 14 mm thick iron and the pot is recycled aluminum. The height of the hearth is 30 cm from the ground. With a radius of 15 cm and a height of the combustion chamber is 10 cm, playing the role of the tunnel that can lead the hot gases to the pot. It is designed on two levels, the first is the combustion chamber with a diameter of 10 cm, and the second allows housing the pot with a thickness of 2 cm. A 13 cm radius pot is designed to fit snugly into the fire pit to prevent leaks. The pot has a lid of the same material as the pot with a radius of 14 cm. The cover covers it during the test to fit without any air intake gap. The biogas arrives at the chimney with a 3.5 mm diameter burner through a pipe from the biodigester. 09 thermocouples are used to take the temperatures which are recorded in the mini data logger; The hearth device is shown in Fig. 2a and that of the entire device from Fig 2b for testing.

2.4 Fuel Quantity Calculation (fired-biogas)

The amount of fuel is obtained by the equation of Bernoulli's theorem in fluids [6] presented in 2.1. With D, the diameter of the burner (mm), p the pressure (kPa), and ρ the density of the biogas ($kg.m^{-3}$). The discharge coefficient 0.9 is obtained from the Bernoulli diagram. The loss coefficient is introduced to account for all inefficiencies of the included flow tube effect $\in [0; 1]$ [7]

$$q_{comb} = Q_{biogas} PCI = 0.036 C d D^2 \sqrt{\frac{p}{\rho}} PCI \quad (2.1)$$

2.5 Numerical Study of the Thermal Efficiency of the Fireplace

The instantaneous efficiency is determined by considering the quotient of all the energies arriving on the kettle as useful energy by the energy of combustion. The energy received by the pot is given by 2.2, avec i are the different pot points.

$$Qu = \frac{m_i Cp_i (T_i - T_0)}{Times} \quad (2.2)$$

T_0 is the value of the initial temperature which is at the same time the ambient value. The yield is now given by:

$$\eta = \frac{Qu}{q_{comb}} 100 \tag{2.3}$$

This function is entered into the program with the same time step as the temperature calculations.

2.6 Thermal Exchange at the Flame (node a)

The conservation equation of energy from burning biogas to heat the combustion chamber is:

$$m_{comb}\mathrm{Cp}_{comb}\frac{dT_a}{dt} = \left[\begin{array}{l} A_1F_{12}\sigma(T_b^4 - T_a^4) + h_1A_1(T_c - T_a) + \\ +A_1F_{14}\sigma(T_d^4 - T_a^4) + U_{1-8}A_1(T_h - T_a) + q_{comb} \end{array} \right] \tag{2.4}$$

The heat produced by the exothermic combustion of the gas is around 900°C, of which the specific heat of the air mixing with the biogas is 0.9536 kJ/kg/℃ [8]. Thus, the equation of this quantity of energy at the level of the burner was calculated at 2.1

2.7 Heat Exchange at the Hearth Wall (node b)

The temperature of the wall of the furnace is close to the flame and calculated according in 2.5.

$$m_{w1}\mathrm{Cp}_{w1}\frac{dT_b}{dt} = \left[\begin{array}{l} A_2F_{21}\sigma({T_a}^4 - T_b^4) + h_1A_2(T_c - T_b) + A_3F\sigma(T_k^4 - T_b^4) + \\ +A_2F_{24}\sigma(T_d^4 - T_b^4) + h_3A_3(T_k - T_b) \end{array} \right] \tag{2.5}$$

2.8 Heat Exchange at the Combustion Chamber (node c)

The heat balance in the combustion chamber is described in equation 2.6.

$$m_{air,1}\mathrm{Cp}_{air,1}\frac{dT_c}{dt} = \left[\begin{array}{l} h_1A_1(T_a - T_c) + h_1A_2(T_b - T_c) + \\ +h_1A_4(T_d - T_c) \end{array} \right] \tag{2.6}$$

2.9 Heat Exchange at the Base of the Kettle (node d)

The base of the firebox is the part in direct contact with the flame and the equation is presented in 2.7

$$m_{pot}\mathrm{Cp}_{pot}\frac{dT_d}{dt} = \left[\begin{array}{l} A_4F_{41}\sigma(T_a^4 - T_d^4) + h_1A_4(T_c - T_d) + \\ +A_4F_{42}\sigma(T_b^4 - T_d^4) + A_5F_{45}\sigma(T_e^4 - T_d^4) + \\ +h_2A_5(T_f - T_d) + A_5F_{47}\sigma(T_g^4 - T_d^4) \end{array} \right] \tag{2.7}$$

2.10 Thermal Exchanges at the Level of the Pot Thickness (node e)

The energy balance between the walls of the pot and the other points is presented by 2.8.

$$m_{pot}\mathrm{Cp}_{pot}\frac{dT_e}{dt} = \left[\begin{array}{l} A_6F_{54}\sigma(T_d^4 - T_e^4) + h_2A_6(T_f - T_e) + \\ +A_6F_{57}\sigma(T_g^4 - T_e^4) + A_7F\sigma(T_k^4 - T_e^4) + \\ +h_3A_7(T_k - T_e) \end{array} \right] \tag{2.8}$$

2.11 Heat Exchange Inside the Pot(node f)

The pot is empty, the air is heated whose energy balance equation is 2.9.

$$m_{air,2}\mathrm{Cp}_{air,2}\frac{dT_f}{dt} = \left[\begin{array}{l} h_2A_5(T_d - T_f) + h_2A_6(T_e - T_f) + \\ +h_2A_8(T_g - T_f) \end{array} \right] \tag{2.9}$$

2.12 Heat Exchange at the Pot Lid (node g)

The heat balance on the lid of the pot is given in 2.10.

$$m_{\text{cover}}\text{Cp}_{\text{cover}}\frac{dT_g}{dt} = \left[\begin{array}{l} h_2A_8(T_f - T_g) + A_8F_{75}\sigma(T_e^4 - T_g^4) + \\ +A_9F\sigma(T_k^4 - T_g^4) + A_8F_{74}\sigma(T_d^4 - T_g^4) + h_3A_9(T_k - T_g) \end{array} \right] \quad (2.10)$$

2.13 Heat Exchange at the Cook Stove Base (node h)

The lining of the base of the fireplace reduces the heat transfer from the burner to the bottom of the fireplace. The energy balance at the bottom of the fireplace, i.e. the most insulated part of the fireplace, is presented in 2.11.

$$\text{m}_{w,2}\text{Cp}_{w,2}\frac{dT_h}{dt} = \left[\begin{array}{l} h_2A_{10}(T_k - T_h) + \\ +A_{10}F\sigma(T_k^4 - T_h^4) \end{array} \right] \quad (2.11)$$

2.14 Determining the Constants

The constants follow the three modes of heat transfer. The conduction considered at the bottom of the focus is given by 2.12.

$$U_{1-8} = \frac{K_{Iron}}{e_{base}} \quad (2.12)$$

With K_{Iron}, the conductivity of iron and e_{base} is the thickness of the firebox.
The form factor to calculate the radiation coefficient between two points i and j are given by 2.13.

$$F_{ij}eq = \frac{1}{\frac{1}{\varepsilon_i} - 1 + \frac{1}{F_{ij}} + \frac{S_i}{S_j}\left(\frac{1}{\varepsilon_i} - 1\right)} \quad (2.13)$$

F_{ij} is the shape factor between the surface of S_i and S_j; ε_i, ε_j are the permissivities of the surfaces. The focus is a black body so ε is 1 and that of the pot (aluminum) is 0.8. After reduction, the radiative exchange coefficient between two bridges becomes 2.14

$$hr_{i-j} = \sigma\varepsilon({T_i}^2 + {T_j}^2)(T_i + T_j) \quad (2.14)$$

The interior of the combustion chamber having the shape of a tube whose $D < L$ is in natural convection. The Nusselt number is given by the relation 2.15

$$Nu_1 = 0.023Re^{0.8}(1 + (D/L))^{(0.7)}0.685^{(1/3)} \quad (2.15)$$

The interior of the empty pot and the surrounding medium are in natural convection [9] so the Nusseelt number is given by the relation 2.16.

$$Nu_2 = 0.54(Gr\,\text{Pr})^{(0.25)} \quad (2.16)$$

The rest of the constants, namely the number of Grassoft Gr, prandlt, thermal expansion β, and the coefficient h of convection are given in 2.17 and 2.18

$$Gr = \frac{g\beta TL^3\rho^2}{\mu^2}; Pr = \frac{\mu Cp}{k} \quad (2.17)$$

$$\beta = 1/T; h = \frac{NuK}{L} \quad (2.18)$$

2.15 Model Validation

The numerical validation consisted in retrieving the author's numerical data and finding a polynomial equation describing these data [10] according to 2.19.

$$y = a_nx^n + a_{n-1}x^{n-1} + a_1x^1 + ... + a_0 \quad (2.19)$$

With a the coefficients and n the degree of the polynomial. This polynomial is implemented under Matlab in order to determine the errors committed on the results with the static formula RMSE (Root Mean Square Error) [11] present in 2.20

$$RMSE = \sqrt{\frac{1}{N}\sum_1^N (y_{\text{exp}}(t_i) - y_{sim}(t_i, \theta))^2} \quad (2.20)$$

yexp are the collected measurements, ysim are the data predicted by the model, θ represents the parameters to be determined and N is the number of measurements.

2.16 Numerical Resolution Procedure

Partial derivative equations are reduced to a system of algebraic equations. The dimensions of the hearth are considered in our calculation code. We proceed to read the coefficients These elements allow us to calculate the first four terms (k1, k2, k3, and k4) from **RUNGE KUTTA** to $T(i)$. Then the temperature value $T(i+1)$ is determined explicitly and so on the program runs over multiple numbers of steps. A total of eight temperatures are to be determined with a **for** loop until the time of $n-1$ before displaying the results. When a solution of the temperatures foresees unsatisfactory results in a region, a modification of the time step is made. With several attempts, a time step of 0.1 second is retained.

3 RESULTS AND DISCUSSION

3.1 Presentation of Results

The figures below show the evolution of all 08 experimental and simulation temperatures as a function of time.

The presented flame temperatures Ta 3a reach their maximum at 900 °C at t= 500 seconds and remain stable. This good result in the quality of the biogas raised 60% of CH_4 according to the work of Jiang [12] whose PCI = 37.78 $kJ.L^{-1}$. The 3.5 mm nozzle burner factor achieves this result by helping to obtain a good air-fuel mixture [13]. The simulated and experimental temperature Tb in Fig. 3b obtain values of 500 °C and 465 °C respectively. This result is favored by the thermal inertia created by the burner thickness of 14mm [14]. Also, the 13 cm diameter of the fireplace allows the flame temperature to touch the walls, increasing its temperature. The Fig. 4a of the combustion chamber temperatures Tc are found at t=10 min at T= 600 °C. The characteristics of the fireplace, namely its thickness, diameter, and height, lead to this result. The height of 10 cm and diameter of 13 cm gives a reduced volume to be heated. Also, the cylindrical shape fits well with the pot avoiding the renewal of the air in the room. The curves in Fig. 4b show a slow evolution to reach values to reach its maximum of Td =500 °C at t = 500s. We find that the heat transfers in the enclosure are influenced by the increase in the heat flux of the burner. Thus, the hot air from the chamber is directed directly to the base of this pot keeping its temperature high at 500°C. Moreover, we see that the temperature of the pot base presented in fig. 4b is not different from that of the flame and this explains a good transfer of heat towards the pot. The temperature curves of the air inside Fig 6a the pot reached a maximum of 220°C. Nevertheless, we notice a difference between this temperature and that of 900°C. This is due either to losses related to the characteristics of the pot (thickness = 2mm, aluminium) or to the continuous renewal of the air within the pot. Looking for a steel pot would yield better results. This result is sufficient to cook any type of meal according to the work of bastista [15]. Bagaya et al [16] on hotplates found a temperature of 408.2 °C and sufficient to prepare any type of food. The curves in Fig. 5a and 5b show respectively the temperatures of the lid and the thickness of the pot. We observe temperatures of 400°C. These results also represent losses dissipated by the pot. This result shows that the pot has low thermal inertia [17]. The Fig. 6b shows the temperatures of the hearth base corresponding to the losses due to the wall of the hearth. The temperature of the loss The in Fig. 6b is around 60 °C which is progress and similar to the work of Sagouong [18] whose result of the parietal loss This 80 °C. This result that the thickness of 14 mm doubled at the base of the hearth made it possible to preserve the temperature within the combustion chamber. This good result makes it possible to reduce the loss of heat which is the problem of open hearths [19]. The experimental temperatures give a good look with the simulated temperatures showing a good prediction of the reduction of heat losses.

3.2 Study Validation

Fig. 7a represents the study of the hottest temperature validation of the hearth between our study and that of sagnoug. Both studies used the RUNGE KUTTA method implemented in MATLAB. The temperature of the Sagouong flame is 750K and 802K for our study at time t = 150s. This observed difference between the two flames is justified by the heat source of the two studies, i.e. the nature of the hearth according to the work of Kausley et al. [20]. Our heat source is biogas fuel and that of Sagouong is coal. This delay, ignition leads to low heat production without forgetting the PCI of coal lower than the PCI of biogas [21]. Also, our black colored steel hearth reduces losses compared to the aluminum author's hearth. The two curves stabilize around 800K after 400 seconds of simulation. The comparison of the calculation error between the two studies is 0.4 K at the end of time t = 800 seconds. We can say that our simulated curve admits the same pace as that obtained by Sagouong [18] proving the effectiveness of the RUNGE KUTTA model. The curves in Fig. 7b show the efficiency of our study and that of Khaushik in a time of 10800 seconds. At t= 0s the η is and 0%, 15% respectively for our study and that of the author. After a time t = 6000s the performance of our study is 50% and that of Kaushik [22]is 49%. It is from this time of 600 seconds that an error deviation (RMSE) of 4% is created with our study. The author's study is superior to our study and this is due to his CFD digital model used, i.e. the ceramic which is the protective insulation of the fireplace. Sowgath showed that CFD is a somewhat simplified structure for analyzing temperature profiles [23]. Also, this author has shown that the results of a study can vary from one software to another due to its flexibility to interact

with subroutines and the consideration of simplifying assumptions. The experimental and simulation figures at the level of the flame show a variation of 900 °C at 850 °C at t=2000s. After this time the two are in agreement with a difference of 3%. For the other experiments, the greatest deviation of 5.75% is observed at the level of temperature (Tc). These differences are due to the phenomenon of the wind sometimes creating a vortex effect in the combustion chamber during the experiment and the renewal of the air in the pot. On the whole, the values predicted by the model are acceptable and provide a solution for the manufacture of stoves.

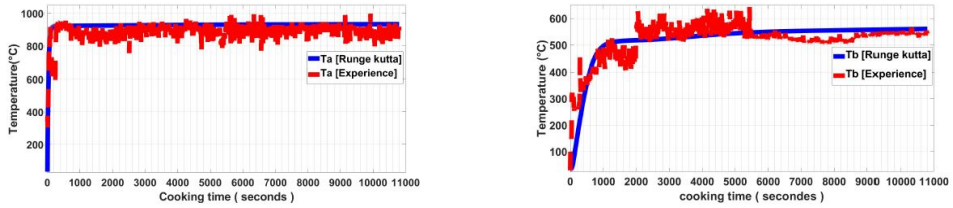

(a) Flame (b) Firebox wall

Fig. 3. Flame temperatures and the thickness of the hearth

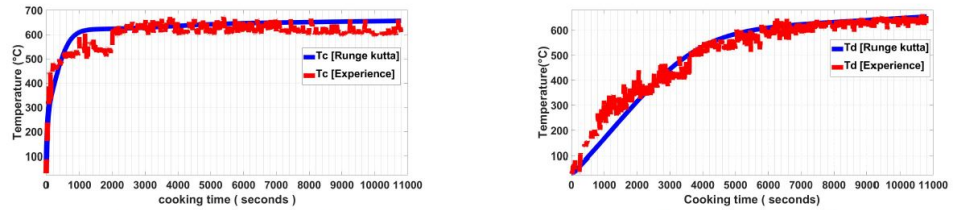

(a) Combustion chamber (b) Pot base wall

Fig. 4. Combustion chamber temperatures and the base of the pot

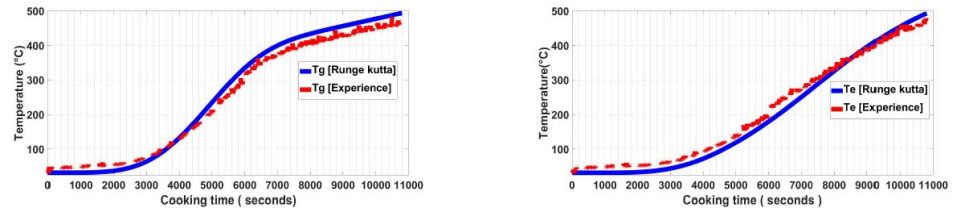

(a) Lid (b) Vertical wall of the pot

Fig. 5. Lid temperatures and the vertical thickness of the pot

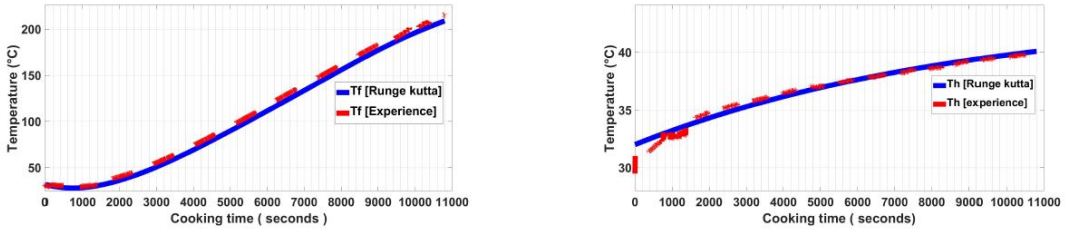

(a) Internal pot temperature (b) Base wall of the fireplace

Fig. 6. Pot internal air temperatures and the firebox base

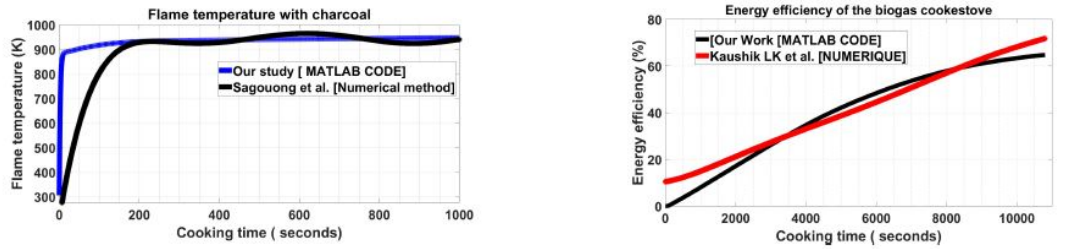

(a) Flame validation (b) Energy efficiency validation

Fig. 7. Flame temperature validation with the numerical model of Sagouong et al and thermal efficiency validation with the Khaushik LK et al model

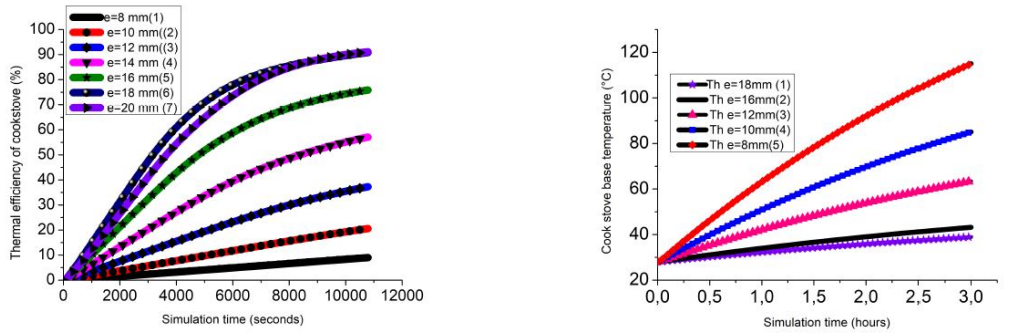

(a) Thermal efficiency (b) Insulation temperature

Fig. 8. Impact of thickness on thermal performance and the firebox base temperature

3.3 Influence of Stove Thickness

Fig. 8b shows the influence of the thickness on the energy loss by the base of the cook stove called the insulation. Fig. 8a presents the thermal efficiency. For a thickness e=14 mm, the efficiency is approximately 65% and the base temperature is 45 °C.

In general, the increase in thickness leads to a gain in thermal efficiency and a reduction in energy losses

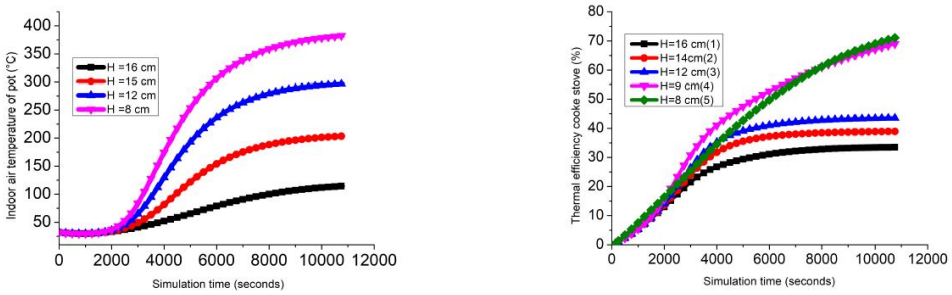

(a) within the pot (b) Thermal efficiency

Fig. 9. Impact of chamber height on internal pot temperature and energy efficiency

to the environment. On the other hand, a thickness of less than 10 mm results in a yield of 25 % and a loss of up to 100 °C. This is because the thickness allows control of the thermal inertia of the cook stove. The conduction studied at point (h) shows that for a thickness of 8 mm the temperature Th is at 115 °C in 03h. This can also be explained by the fact that the heat transfers by conduction between the center of the hearth enclosure and the wall of the hearth becomes weak if the thickness of the hearth is high and strong if the thickness becomes more and more strong. For a thickness e = 18 mm the energy efficiency reaches 90% which means a quantity of energy is sent to the pot. The optimal thickness is e=18mm beyond which no energy is observed as shown in the Fig. 8a.

3.4 Influence of Combustion Chamber Height

The curves in Fig. 9 show the evolution of the temperature in the kettle and the efficiency as a function of time.

With an increase in the height of the combustion chamber, the flame does not reach the bottom of the pot. This results in a large combustion chamber surface area, which reduces wall temperatures. Therefore, the height leads to a decrease in thermal efficiency. With a height H = 14 cm the $\eta = 40\%$, H = 10 cm $\eta = 65\%$, and H=10 $\eta = 70\%$ the temperature. This shows the lower the height, the closer the pot is to the flame, therefore a high thermal gradient (Ta=900°C) is recovered by the pot. The optimal height is H= 9 cm beyond that, there is no longer any gain illustrated in curve 9b. This means from 9 cm all the energy detectable by the pot is reached.

4 CONCLUSION

This work, the objective of which was to propose a prototype of an energy efficient- biogas stove, has yielded results. The cook stove studied numerically under **MATLAB** $R2021b$ gave results in line with the experiment. The biogas flame reached a temperature of 900 °C and the combustion chamber around 600 °C.The temperature of the interior air in the pot reached is 220 °C which can cook a meal according to the work of Shen [24]. The instantaneous thermal efficiency of the fireplace is 65%. It appears from this study that the optimal height of the combustion chamber is 09 cm and the optimal thickness is 18 mm. Numerical validation with the literature [22] gives agreement with a maximum car of 6%. This result is better compared to Bagaya's study [16] on the biogas stove, for which $\eta = 55\%$, therefore acceptable according to the literature [25]. However, the energy performance of the home will drop in a busy kitchen, but its adoption by a cooking stove is already an important step in reducing wood cutting in Burkina Faso.

ACKNOWLEDGEMENT

This article follows research supported by the National Biodigesters Program of Burkina Faso (PNB-BF) and International Scientific Program (ISP),University of Uppsala, Sweden through project BUFO1 funding. Also, the Embassy of France in Burkina Faso is recognized for its financing of Bagaya Noufou's research stay in Paris Saclay University.

COMPETING INTERESTS

The Authors have declared that no competing interests exist.

REFERENCES

[1] Vianello M. The Energy Situation in Goudoubo Refugee Camp, Burkina Faso; 2017.

[2] Faso B. Cinquième Recensement Général de la Population et de l'Habitation du Burkina Faso; 2022.

[3] Hausman B. Développement d ' un digesteur de surface pour l ' intégration alternative du biogaz au Burkina Faso; 2018.

[4] Whitman T, Nicholson CF, Torres D, Lehmann J. Climate change impact of biochar cook stoves in western kenyan farm households. Environmental Science and Technology. 2011;45(8):3687–3694.
Available: https://doi.org/10.1021/es103301k

[5] Ceballos, Gerardo et al. "Accelerated Modern Human-Induced Species Losses: Entering the Sixth Mass Accelerated Modern Human – Induced Species Losses: Entering the Sixth Mass Extinction; 2015.

[6] Kurchania AK, Panwar NL, Pagar SD. International Journal of Sustainable Energy Design and performance evaluation of biogas stove for community. 2010;29(2):116–123.
Available: http://www.tandfonline.com/action/journalInformation.journalCode=gsol20

[7] Petro LM, Machunda R, Tumbo S, Kivevele T. Theoretical and Experimental Performance Analysis of a Novel Domestic Biogas Burner; 2020.

[8] Augustin LM, Vertomene ST, Bernard NN, Sadiki A, Haddy MK. A New Perspective on Cooking Stove Loss Coefficient Assessment by Means of the Second Law Analysis. 2022;1–27.

[9] Zube NG, Zhang X, Li T, Le T, Li C, Guerlet S, Tan X. Radiative-dynamical Simulation of Jupiter's Stratosphere and Upper Troposphere. The Astrophysical Journal. 2021;921(2):174.
Available: https://doi.org/10.3847/1538-4357/ac1e95

[10] Tampango Y, Potier-ferry M, Koutsawa Y, Tampango Y, Potier-ferry M, Koutsawa Y. Une méthode sans maillage basée sur la résolution de l ' EDP par séries de Taylor To cite this version: HAL Id: hal-00592826; 2011.

[11] Guermoui M, Abdelaziz R, Gairaa K, Djemoui L, Benkaciali S. New temperature-based predicting model for global solar radiation using support vector regression. International Journal of Ambient Energy. 2022;43(1):1397–1407.
Available: https://doi.org/10.1080/01430750.2019.1708792

[12] Jiang X, Mira D, Cluff DL. The combustion mitigation of methane as a non-CO2 greenhouse gas. Progress in Energy and Combustion Science. 2018;66:176–199.
Available: https://doi.org/10.1016/j.pecs.2016.06.002

[13] Devi S, Sahoo N, Muthukumar P. Combustion of biogas in Porous Radiant Burner: Low emission combustion.Energy Procedia. 2019;158:1116–1121.
Available: https://doi.org/10.1016/j.egypro.2019.01.276

[14] Powell T, O'Donnell R, Hoffman, Kumar R. Experimental investigation of the relationship between thermal barrier coating structured engine combustion. International Journal of Engine Research. 2021;22(1):88–108.
Available: https://doi.org/10.1177/1468087419843752

[15] Batista C. de S, dos Santos JP, Dittgen CL, Colussi R, Bassinello PZ, Elias MC, Vanier NL. Impact of cooking temperature on the quality of quick cooking brown rice. Food Chemistry. 2019;286:98–105.
Available: https://doi.org/10.1016/j.foodchem.2019.01.187

[16] Bagaya N, Ouédraogo I, Windé D, Koumbem N, Sandwidi GW, Kieno FP. Energy Performance Analysis of B1-3 . 5mm Burner Model of Fasobio-15 Biodigester Biogas Cookstoves. 2021;25(7):11–21.
Available: https://doi.org/10.9734/PSIJ/2021/v25i730268

[17] Huang Y, Risha GA, Yang V, Yetter RA. Effect of particle size on combustion of aluminum particle dust in air. Combustion and Flame. 2009;156(1):5–13.
Available: https://doi.org/10.1016/j.combustflame.2008.07.018

[18] Sagouong JM, Tchuen G. Mathematical modelling of traditional stoves using the Thermal Network

Approach; 2018.
Available: https://doi.org/10.14445/22315381/IJETT-V58P201

[19] Gandigude A, Nagarhalli M. ScienceDirect Simulation of Rocket Cook-Stove Geometrical Aspect for its Performance Improvement. Materials Today: Proceedings. 2018;5(2):3903–3908.
Available: https://doi.org/10.1016/j.matpr.2017.11.645

[20] Kausley, Shankar B, Aniruddha B Pandit. "Modeling of Solid Fuel Stoves." Fuel. 2010;89(3): 782–91.
Available: http://dx.doi.org/10.1016/j.fuel.2009.09.019.

[21] Russell A, et al. Using Forests to Enhance Resilience to Climate Change: The Case of the Wood-Energy Sector in Burkina Faso; 2013.

[22] Kaushik LK. Performance and Feasibility Assessment of Porous Radiant Burner Aided Cook-stoves for LPG , Biogas and Waste Cooking Oil Fuels Doctor of Philosophy by Department of Mechanical Engineering Indian Institute of Technology Guwahati Department of Mechanical En; 2019.

[23] Sowgath, Tanvir, Mominur Rahman, Sabbir Ahmed Nomany, and Nazmus Sakib. "CFD Study of Biomass Cooking Stove Using Autodesk Simulation CFD to Improve Energy Efficiency and Emission Characteristics. 2015;45:1255–60.

[24] Shen G, Hays MD, Smith KR, Williams C, Faircloth JW, Jetter JJ. Evaluating the Performance of Household Liquefied Petroleum Gas Cookstoves Evaluating the Performance of Household Liquefied Petroleum Gas Cookstoves; 2017.
Available: https://doi.org/10.1021/acs.est.7b05155

[25] Grimm M. Impact Evaluation of Improved Stove Use among Dolo-beer Breweries in Burkina Faso – FAFASO. 2014;2013:1–31.

Peer-review history:
The peer review history for this paper can be accessed here:
https://www.sdiarticle5.com/review-history/94286